

Seismic response prediction and modeling considerations for curved and skewed concrete box-girder bridges

Karthik Ramanathan¹, Jong-Su Jeon^{*2}, Behzad Zakeri³, Reginald DesRoches²
and Jamie E. Padgett⁴

¹*AIR Worldwide, 131 Dartmouth Street, Boston, MA 02116, USA*

²*Civil and Environmental Engineering, Georgia Institute of Technology, 790 Atlantic Drive, GA 30332, USA*

³*Civil and Environmental Engineering, University of California, Irvine, CA 92697, USA*

⁴*Civil and Environmental Engineering, Rice University, 6100 Main Street, Houston, TX 77005, USA*

(Received January 8, 2015, Revised October 20, 2015, Accepted October 30, 2015)

Abstract. This paper focuses on presenting modeling considerations and insight into the performance of typical straight, curved, and skewed box-girder bridges in California which form the bulk of the bridge inventory in the state. Three case study bridges are chosen: Meloland Road Overpass, Northwest Connector of Interstate 10/215 Interchange, and Painter Street Overpass, having straight, curved, and skewed superstructures, respectively. The efficacy of nonlinear dynamic analysis is established by comparing the response from analytical models to the recorded strong motion data. Finally insights are provided on the component behavioral characteristics and shift in vulnerability for each of the bridge types considered.

Keywords: straight, curved, skewed box-girder bridge; numerical model; model validation; component behavior; fragility

1. Introduction

The 1971 San Fernando, 1989 Loma Prieta, and 1994 Northridge earthquakes in California motivated significant research on the seismic response, analysis, and design of bridges. These earthquakes resulted in major damage or collapse to many bridges that were at least nominally designed for seismic forces (Basoz and Kiremidjian 1998, Priestley *et al.* 1996). Following these earthquakes, elastic bridge design philosophy was modified with a major focus on ductility and inelasticity and special attention to detailing aspects (Yashinsky and Ostrom 2000).

Box-girder bridges constitute the bulk of the bridge inventory in California accounting for roughly 20% of the overall bridge inventory. These bridges experienced different levels of damage in these seismic events. Seventy six bridges and several viaducts were damaged during the Loma Prieta earthquake, and 233 in the case of the Northridge event (Basoz and Kiremidjian 1998). The 1994 Northridge earthquake resulted in collapse of several bridges, all of which were multi-span continuous concrete box-girder bridges. The vulnerability was attributed to the high skew, irregularities in the substructure stiffness, and inadequate seat widths (Fenves and Ellery 1998,

*Corresponding author, Postdoctoral Fellow, Ph.D., E-mail: jongsu.jeon@gatech.edu

Moehle *et al.* 1995). The presence of superstructure curvature and skewness further exacerbated the level of damage in some of these bridges. The presence of curves and skewed supports in the bridge superstructure results in complex vibration modes due to predominance of torsion with respect to the vertical axis of the bridge. This out-of-phase motion may increase the deformation demand on several bridge components such as deck, column, abutments, and bearings. In particular, when these bridges with expansion joints at the abutments or intermediate hinges are subjected to varying levels of seismic excitations, additional hinge openings on the either side of deck due to the torsional effect may cause the potential for toppling of the bearing or potential unseating of the span. In addition, pounding between adjacent frames, occurring at the opposite side of the hinge opening, results in structural damage including concrete spalling at the hinges and create undesirable forces in the adjacent frames. Therefore, proper characterization of the force deformation response at the component level plays a major role in response prediction at the local member level and global bridge system level.

However, current bridge design specifications in the United States do not have any guidelines regarding seismic performance assessment of curved and skewed concrete box-girder bridges. Furthermore, very few studies focused on the behavior and modeling considerations of curved and skewed bridges and the relative shift in component vulnerability in these bridge types in comparison to straight and non-skewed bridges. As a result of the relative importance of the class of box-girder bridges and its abundance in the state inventory, it is imperative to accurately model and predict their response. Moreover, a better understanding of the effect of skew and curvature will result in the ability to better model these characteristics, and ultimately improve the capability of determining a number of principal effects of earthquakes such as traffic disruption, recovery cost and downtime as well as lead to robust design and retrofitting practices.

The next section presents a concise literature survey on the modeling and behavioral aspects of curved and skewed bridges to date. Given the lack of guidelines on modeling strategies for these bridge components, this paper makes an attempt to present modeling considerations and insight into the performance of typical straight, curved, and skewed box-girder bridges in California which form the bulk of the bridge inventory in the state. Three case study bridges are chosen for each of the aforementioned types: Meloland Road Overpass, Northwest Connector of Interstate 10/215 Colton Interchange, and Painter Street Overpass, with straight, curved, and skewed superstructure geometries, respectively. The fundamental objective of this study is to provide detailed information about the finite element (FE) modeling approach required to adequately capture the response of this bridge type and to determine the efficacy of nonlinear dynamic analysis to predict the response recorded in earthquakes. The responses from the generated FE models are compared with recorded sensor data made available through a network of sensors instrumented on the case study bridges. A nonparametric evaluation technique is also employed to identify the bridge vibration periods using recorded sensor data. Finally insights are provided on the component behavioral characteristics and shift in seismic vulnerability among components for each of the bridge types considered with variable superstructure geometric configurations.

2. Past studies on predicting bridge response to seismic excitation

Ever since the 1971 San Fernando and 1989 Loma Prieta earthquakes, there has been an increased effort to understand the behavior of multi-span bridges. These historic events led to the establishment of a wide network of sensors on a large number of bridges in California by the

Center for Engineering Strong Motion Data (CESMD) (Haddadi *et al.* 2008).

Early studies on the seismic response prediction of bridges focused on the performance of the Meloland Road Overpass during the 1979 Imperial Valley earthquake. Several researchers (Douglas and Richardson 1984, Douglas *et al.* 1990, Werner *et al.* 1987, Zhang and Makris 2002) utilized the large amplitude response recorded during the 1979 Imperial Valley earthquake in validating or calibrating FE models. In addition, Werner *et al.* (1987) and Gates and Smith (1982) used system identification techniques to determine vibration properties of the bridge. Wilson and Tan (1990a, b) proposed an equivalent linear spring model to represent the transverse and vertical stiffness of the abutments and compared their responses with recorded sensor data pertaining to the earthquake from the bridge. The studies concluded that abutments and embankments significantly affected the response of the bridge. Kwon and Elnashai (2008) used a multiplatform analysis including soil structure interaction and compared the response of the bridge to the results from system identification techniques using recorded data on the bridge from the earthquake.

For curved bridges, DesRoches and Fenves (1997) focused on the global response correlation using recorded sensor data with the analytical model for the Northwest Connector of Interstate (I) 10/215 Colton Interchange using nonlinear time history analysis (NLTHA). These authors employed elastic beam-column models for most bridge components except for the intermediate hinges. This could result in underestimating the column response if the columns experience nonlinear response. Huang and Shakal (1995) provided a comprehensive interpretation of the recorded sensor data on the I10/215 Interchange bridge along with recommendations for bridge component modeling. Fenves and Ellery (1998) evaluated the earthquake response of the Separation and Overhead bridge that partially collapsed during the 1994 Northridge earthquake. The analytical model represents intermediate hinge opening and closing, inelastic response characterization of columns, restrainers, and abutments.

In the case of skewed bridges, several studies examined the dynamic response of the Painter Street Overcrossing. While few studies interpreted the dynamic response characteristics by comparing the natural frequency and mode shape of different analytical models for six earthquakes between 1980 and 1987 (Maroney *et al.* 1990, Fenves *et al.* 1992), other studies (Sweet and Morrill 1993, Goel and Chopra 1997, McCallen and Romstad 1994, Zhang and Makris 2002) focused on varying levels of sophistication of analytical modeling procedures in trying to capture the dynamic response of the Painter Street Overcrossing to seismic input. Although these studies did not focus on skew effects explicitly, they underscored the importance of component modeling approaches when torsion dominates the overall response of skewed bridges. Bjornsson *et al.* (1998) found that the maximum relative abutment displacement increases with the increase of skew angle, especially between 45° to 60°. Meng and Lui (2000) demonstrated that the effect of boundary conditions is more significant than the effect of skew angle in dynamic response of a bridge. Bignell *et al.* (2005) revealed that the coupling displacement associated with skewness results in developing some failure modes in skew bridges that might not be seen in non-skew bridges such as failure of bearings at the abutments of bridges with higher skew angles. Dimitrakopoulos (2010) highlighted the predominance of vulnerable skewed bridges worldwide and importance of characterizing and assessing their susceptibility to damage. Seismic response of three span continuous skewed box-girder bridges was studied by Abdel-Mohti and Pekcan (2008) for 0° to 60° skew angle with different boundary conditions (with or without shear keys) and analytical models for bridges. It was concluded that for bridges with skew angle more than 30°, FE models should be adopted and boundary conditions can have a significant effect on pushover analyses and choice of pushover load profile. Kaviani *et al.* (2010) examined the response of two

and three span skewed box-girder bridges with single- and multi-column bents. The effects of shear keys and bearing pads were eliminated in their modeling approach. The findings suggested that an increase in abutment skew angle amplifies deck rotation, particularly in bridges with single column bents. It was also concluded that abutment longitudinal displacement and column drift are less sensitive to bridge skew angles in comparison to abutment transverse displacement and deck rotation.

3. Description and analytical modeling procedure of case study bridges

This section provides a detailed description of the three case study bridges along with information about the analytical modeling procedure.

3.1 Meloland Road Overpass

The Meloland Road Overpass is a two span reinforced concrete box-girder bridge built in 1971 located in Southern California. The bridge has two equal spans 31.7 m in length and 10.4 m wide supported on a single column bent 6.4 m high integral with the superstructure that frames into diaphragm abutments at its ends. The bridge is instrumented with twenty six channels of accelerometers and the 1979 Imperial Valley earthquake is the strongest earthquake to strike the bridge with peak ground acceleration (PGA) values of 0.32 g, 0.30 g, and 0.23 g in the longitudinal, transverse, and vertical directions, respectively.

Fig. 1 shows the layout of the bridge along with details of the analytical modeling procedure. A three dimensional spine model of the bridge is created in the FE platform OpenSees (McKenna *et al.* 2010). The deck response is simulated using elastic beam-column elements and the columns are modeled using fiber-type beam-column elements and lumped masses. Fiber defined cross-sections help in capturing the spread of plasticity in the element and at the same time facilitates the specification of different properties for cover and core concrete to account for the effects of confinement and ductility. The model of Mander *et al.* (1988) was used to account for the enhanced compressive strength and ductility of core concrete due to confinement. In order to check shear failure in the bridge columns, a simple elastic perfectly plastic model is implemented at the ends of the columns with the shear capacity calculated as prescribed by ACI 318-08 (2008)

$$V_{bent} = 0.29\sqrt{f'_c}(0.8D^2)\sqrt{1 + \frac{0.29N_u}{A_g} + \frac{A_v f_y (0.8D)}{s}} \quad (1)$$

where f'_c is the concrete compressive strength (MPa), D is the column diameter (mm), N_u is the column axial load (N), A_g is the gross cross-sectional area (mm²), A_v is the area of transverse reinforcement (mm²), f_y is the steel yield strength (MPa), and s is the transverse reinforcement spacing (mm). It is important to note that although this check was implemented, the bridge columns in all the three case study bridges were dominated by flexural behavior, as will be discussed in the next section.

Nonlinear translational springs are used to capture the response of the abutments in the longitudinal and transverse directions. The longitudinal abutment response is comprised of active and passive actions. Soil and piles contribute to the passive (compressive) resistance of the abutments while the active (tensile) resistance is assumed to be provided by the piles alone. The

transverse response of the abutment is assumed to be characterized solely by the piles.

The hyperbolic soil model proposed by Shamsabadi *et al.* (2010) is used to capture the response of the abutment backwall soil in passive action. The model is based on experimental testing of bridge abutments with typical cohesionless and cohesive backfill soils in passive response (Stewart *et al.* 2007, Romstad *et al.* 1995). The test results were then extended to develop closed form solutions for the abutment backfill soil response for a range of backfill heights based on a series of analyses using the limit equilibrium method that implements mobilized logarithmic spiral failure surfaces coupled with a modified hyperbolic soil stress strain behavior. The initial stiffness of the soil is assumed to be 20.3 kN/mm and the ultimate passive resistance is 0.326 kN per mm width of the abutment back wall consistent with the abutment backfill soil present at the bridge location. Zero-length springs characterized by nonlinear soil behavior are used to capture the response

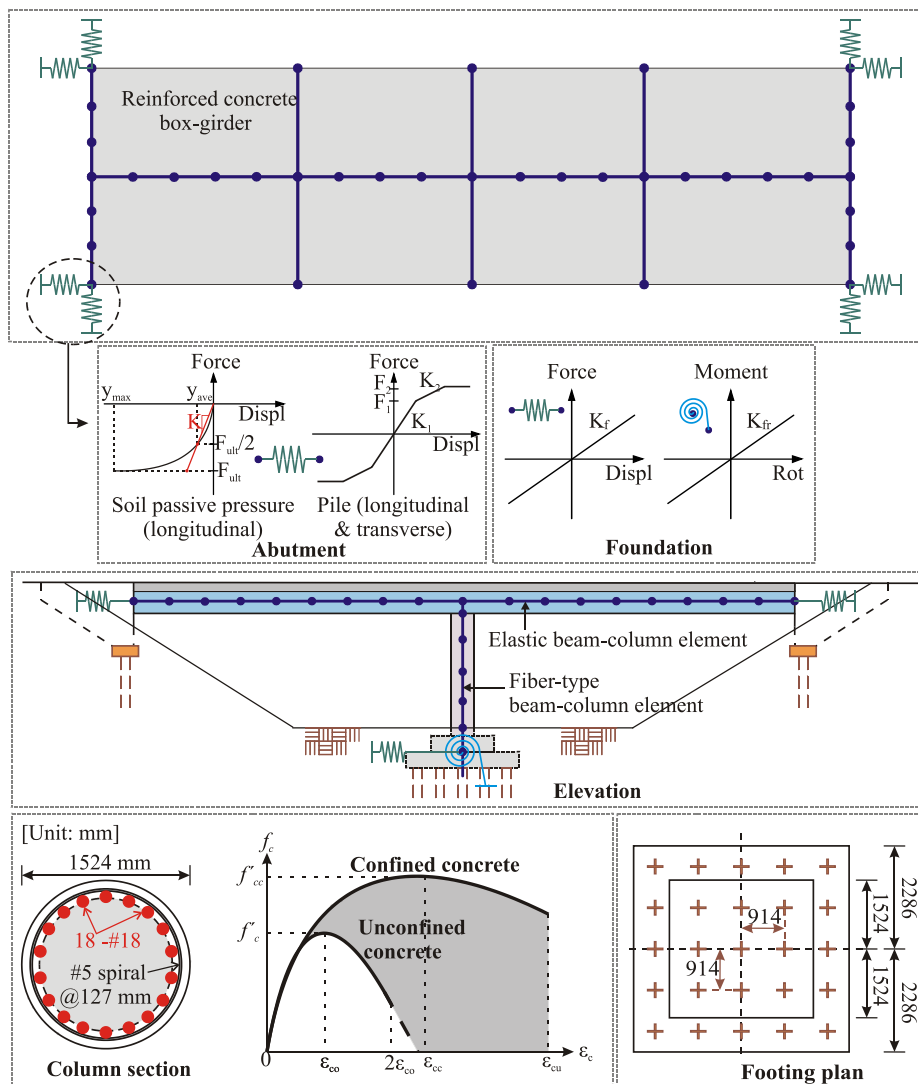


Fig. 1 Details of the Meloland Road Overpass analytical modeling procedure

of the abutment soil. The response of piles was described by a trilinear force-deformation relationship stemming from the recommendation of Choi (2002) assuming a translational stiffness of 7 kN/mm/pile per Caltrans (2010). It is important to note that the primary focus of this paper was to provide simplified yet accurate modeling solutions and henceforth explicit modeling of the soil structure interaction was not considered. However, the stiffness of the soil and pile springs were calibrated to match the response from the recorded sensor data and this system provides computational efficiency to support not only practical design assessment but also numerous simulations required of a probabilistic vulnerability assessment.

Lumped translational and rotational springs at the base of the column are used to capture the behavior of pile foundations. The composite behavior is evaluated based on geometry and pile group effects (Ma and Deng 2000). 15% Rayleigh damping in the first two modes was considered in this study following the recommendation of Zhang and Makris (2002).

3.2 Northwest Connector (I10/215 Colton Interchange)

The Northwest Connector constructed in 1969 is a curved bridge which carries two lanes of traffic from eastbound I-10 to northbound I-215 at an interchange in Colton, California. The connector is a 774.2 m long, curved, concrete box-girder bridge with sixteen spans supported on single column bents and diaphragm abutments. Beginning at Abutment 1, the alignment is composed of three segments: a curved segment 310.3 m long and 365.8 m radius, a curved segment 386.5 m long and 396.2 m radius, and a 77.4 m straight segment ending at Abutment 17. The central portion of the bridge has a vertical curve of 274.3 m radius with a maximum profile grade of 4.74%. The Northwest Connector was one of the first curved bridges to be instrumented by CESMD and has strong motion data recorded during the 1992 Landers earthquake.

As illustrated in Fig. 2, the superstructure consists of five intermediate hinges (Hinge 3, Hinge 7, Hinge 9, Hinge 11, and Hinge 13) and six frames of conventional reinforced and prestressed concrete box-girders, which rest on elastomeric bearing pads at the hinges. Both types of concrete box-girders are similar except for the web thickness of the interior cells. The as-built flared octagonal columns are 1.68 m×2.44 m in dimension and the bent cap is 2.90 m wide and 2.44 m deep. The foundations for the column bents consist of a pile cap and reinforced concrete piles ranging from 6.40 m to 15.24 m in depth. At the diaphragm abutments, the box-girder is integral with a 3.96 m high backwall and the tapered wing walls are 5.49 m long. Abutments 1 and 17 have nine 22.95 m long piles and seven 13.10 m long piles, respectively. The five intermediate hinges have seat widths ranging from 0.81 to 0.91 m. Shear keys were used to inhibit the relative transverse displacement whose sides have a 6.4 mm joint filler. In 1991, the connector underwent column and footing retrofit along with replacement of the cable restrainers. The columns were retrofit using a 12.7 mm thick elliptical steel jacket, while the footings were strengthened by increasing their size, addition of steel jacket and provision of supplemental steel piles. The retrofitted bridge was considered for the analytical modeling procedure and FE model validation using the 1992 Landers earthquake since the strong motions were recorded on the retrofitted bridge.

Fig. 3 shows the analytical modeling procedure of the Northwest Connector. As in the case of the Meloland Road Overpass, OpenSees was chosen as the FE analysis platform. The superstructure is modeled as a spine with elastic beam-column elements as it is expected to remain elastic during seismic events. The effective stiffness for reinforced concrete box-girders (Frames 1, 3, 5, and 6) are based on 75% of the gross stiffness to account for concrete cracking (Caltrans

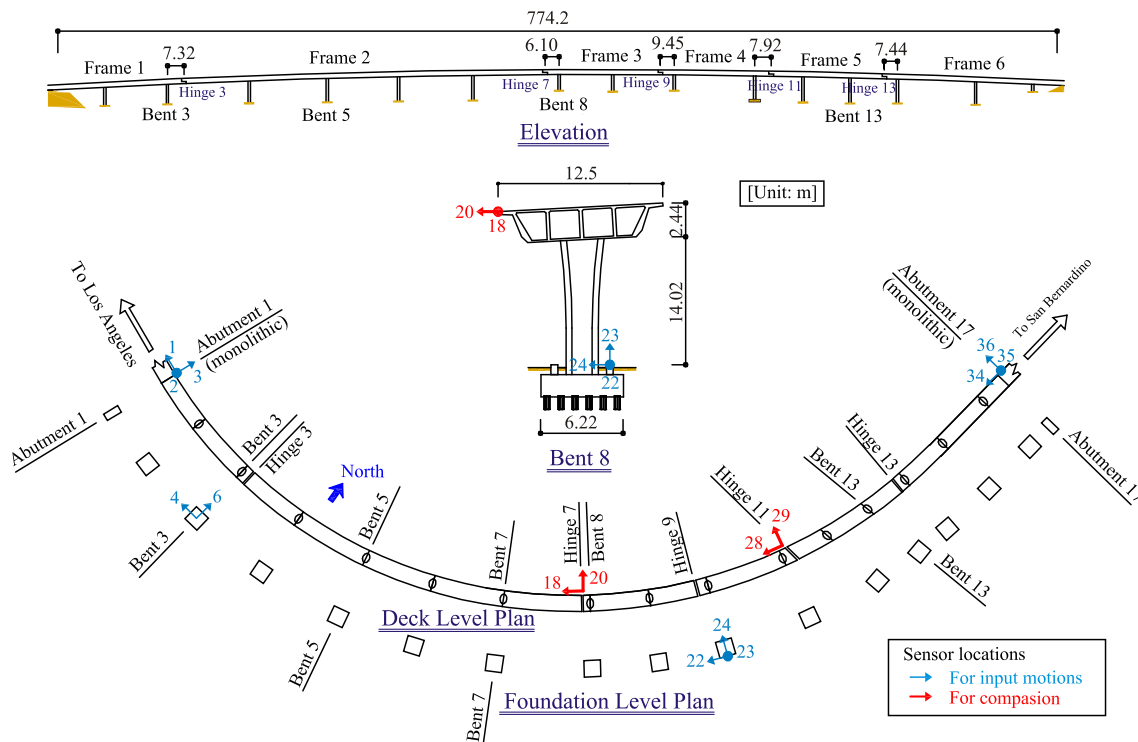


Fig. 2 Layout and sensor locations for the Northwest Connector-Colton Interchange

2010) while pre-stressed concrete girders (Frames 2 and 4) are modeled for the full gross-stiffness as these elements are crack free. The effective superstructure width is reduced near the bent caps following the recommendation of Priestley *et al.* (1996), Caltrans (2010). The transverse deck elements are modeled as rigid, massless beam elements to represent the diaphragm and intermediate hinges and account for the twisting of the box-girder. Buckle *et al.* (2006) emphasized the necessity to account for the rotational mass moment of inertia along the bridge axis for curved bridges. Henceforth, this lumped rotational mass was converted into 40% of translational mass at the both ends of the transverse beam elements, because of the inability to consider the direct application of the lumped mass moment of inertia along the local axis in OpenSees. This ratio is the total rotational mass divided by the deck width (moment arm). The remainder of the mass is lumped at the centerline along the bridge axis.

The columns are modeled using fiber-type beam-column elements and rigid links at the superstructure-column connections and the footing-column connections to transfer all of the moment. As in the previous case, the Mander model (1988) is used to account for the enhancement of compressive strength and ductility of core concrete. In addition, for retrofitted columns, the confinement due to elliptical steel jackets is accounted for based on the recommendations of Priestley *et al.* (1994). The abutment backfill soil response is simulated using a multi-linear curve equivalent to the hyperbolic soil model (Shamsabadi *et al.* 2010). The horizontal response of abutment piles is modeled using zero-length springs with a trilinear force deformation curve assuming a stiffness of 7 kN/mm/pile (Caltrans 2010). For foundation piles, the horizontal and rotational responses are simulated using linear springs based on the equations presented in Ma and

Deng (2000) and vertical spring stiffness is considered 175 kN/mm (Choi 2002).

The intermediate hinge model consists of contact elements that account for the pounding effect between adjacent decks, cable restrainer with an initial slack and elastomeric bearing. These component responses are replicated by considering zero-length nonlinear springs characterized by the respective component force-deformation characteristics, as shown in Fig. 3. The pounding element is defined using the model of Muthukumar and DesRoches (2006), modeled as a nonlinear compression-only element with a gap, and the restrainer is modeled as a nonlinear tension-only

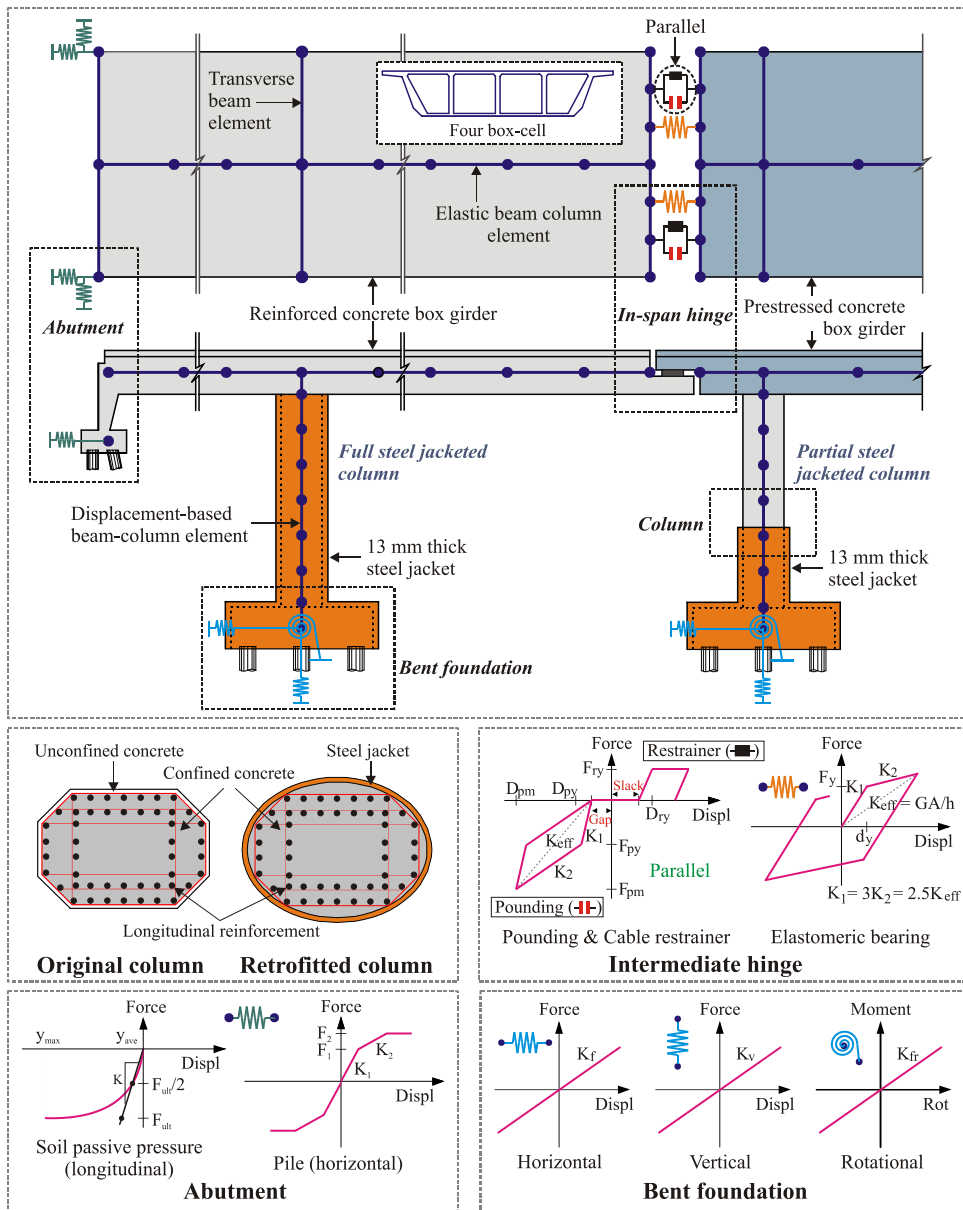


Fig. 3 Details of the Northwest Connector analytical modeling procedure

element with an initial slack. The stiffness of the cable restrainers is given by EA/L where E , A , and L are the elastic modulus and total cross sectional area, and length, respectively, of the restrainer cables, with values of 69 GPa, 142 mm², and 6.1 m, respectively. The total yield force is based on an individual cable yield force of 174 kN. Since both elements are involved in the longitudinal response of the intermediate hinge, for simplicity, the pounding element is combined in parallel with the restrainer element. In compression, the pounding stiffness is very high once the initial gap has closed, resulting in a restraint in the compressive movement, while the restrainer stiffness is activated in tension following slack elimination, resulting in reducing the tensile movement. In addition, the gap closure produces no or little longitudinal compressive deformation of elastomeric bearings. The elastomeric bearing pads with shear modulus of 1 MPa are modeled using a bilinear element proposed by Naeim and Kelly (1999). The hinge gaps and slack in the restrainer cables are the same as those adopted by DesRoches and Fenves (1997). Since the gap between shear key and upper deck is only a quarter inch, the relative transverse displacement is constrained to be zero in the analytical model. Furthermore, the relative vertical displacement and twisting at the hinge are also constrained to be zero.

3.3 Painter Street Overpass

The Painter Street Overpass is located on Highway 101 in Rio Dell, California, is a monolithic, cast-in-place skewed bridge built in 1976, and consists of prestressed concrete box-girders supported on a two-column bent framing into end diaphragm abutments. This bridge has two spans measuring 44.5 m and 36.3 m in length. The bridge has a 39° skew angle between the centerlines of bent and deck. The bridge columns are circular in cross section with 1.52 m in diameter and flare to a width of 2.74 m at the top. While the east abutment is monolithic with the foundation, the west abutment is located on a bearing pad on top of the pile cap. Both the columns and abutments are founded on piles. A longitudinal shear key is located at a gap of 25 mm at the right abutment and the transverse ones are located on either side of the abutment to prevent additional displacement of the bridge during seismic excitation. The expansion joint is filled with expanded polystyrene and protected with angle-shaped neoprene to prevent the entry of soil and water into the joint. The bridge was instrumented in 1977 with 17 channels of accelerometers.

Global seismic behavior of a skewed bridge is affected by a number of factors, including the skew angle, column ductility, shear keys, and characteristics of the seismic source (Shamsabadi *et al.* 2010) among others. Fig. 4 shows details of the analytical modeling procedure adopted for the Painter Street Overpass. As in the previous two case study bridges, the columns of the Painter Street Overpass are modeled using fiber-type beam-column elements while the deck is modeled as a linear elastic section anticipating elastic response during seismic excitation.

Abutments tend to dominate the overall bridge response in the case of short and skewed bridges, and capturing their behavior is important (McCallen and Romstad 1994). Since the abutments are monolithic with the deck, they are consequently modeled using vertical rigid elements. As in the case of the Meloland Road Overpass, the soil abutment interaction is modeled using the hyperbolic soil model proposed by Shamsabadi *et al.* (2010). An average value of 14.5 MPa is implemented as the initial stiffness for passive pressure with maximum deformation restricted to 10% of the back wall height. The hyperbolic curve is subsequently approximated by a multi-linear curve using parameters specified by Choi (2002). Zero-length elements characterized by this force deformation relationship are located at the top of the abutments in the longitudinal direction. The bridge has two wing walls at each end which significantly influence the seismic

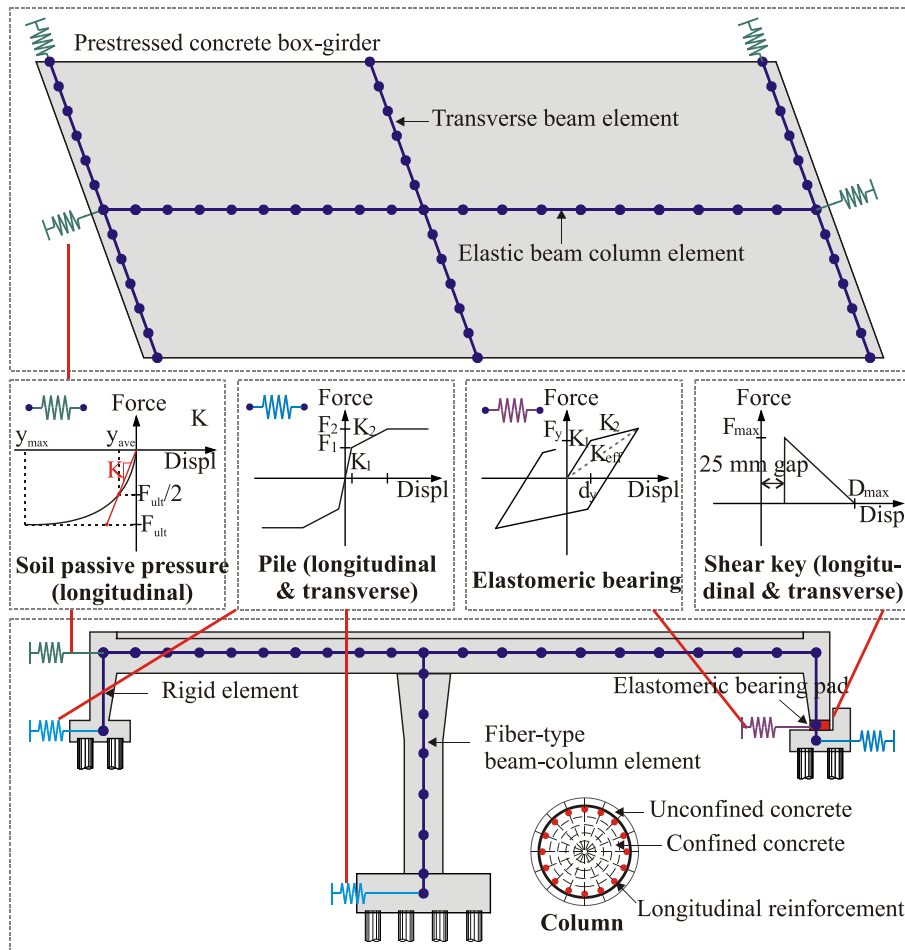


Fig. 4 Details of the Painter Street Overpass analytical modeling procedure

response of the bridge. As a result, the wing wall effectiveness and participation coefficient values equal to $2/3$ and $3/3$, respectively, are used following the recommendations of Maroney *et al.* (1994). The passive response of the soil behind the wing walls is modeled in the same fashion as in the case of the abutment back wall. Zero-length elements characterized by the force-deformation response of the wing wall soil are assigned to the analytical model in the transverse direction. Pile elements are modeled in the same fashion as in the case of the previous two bridges.

As previously mentioned, the west abutment has one shear key in the longitudinal direction and two shear keys in the transverse direction at a 25 mm gap. Their force-deformation response is modeled using a trilinear curve following the Caltrans - UCSD field experiments (Megally *et al.* 2002). The zero-length elements capturing the response of the shear keys are assembled in series with pile elements and a gap element. In the longitudinal direction, the gap element is modeled using an initial stiffness equal to 15% of shear key stiffness. The response of the bearing pads is modeled using a bilinear model governed by friction with an assumed value of coefficient of friction between concrete and the neoprene equal to 0.4 (Caltrans 2010). For the east abutment where the abutment and foundation are monolithic, a conservative approach is taken and the

contribution of piles alone is considered in either direction. The foundation system is represented by translational linear springs in the longitudinal and transverse directions. The rotational stiffness of the foundation is neglected since the columns are pinned to the pile cap.

4. Finite element model validation

The aim of this study is to determine the efficacy of detailed nonlinear analytical modeling and dynamic analysis procedures to predict the response of box-girder bridges with complex geometries during earthquakes. This section presents the results of modal analysis for each of the case study bridges. Comparison between the results of NLTHA on the analytical bridge models and the recorded sensor data for certain scenario earthquakes that each bridge is subjected to are also presented. The 1979 Imperial Valley earthquake is used in the case of the Meloland Road Overpass while the 1992 Landers earthquake is used in the case of the Northwest Connector. The 1992 Cape Mendocino/Petrolia earthquake is used for validating the Painter Street Overpass. Spectral analysis, a non-parametric technique to determine the vibration periods using the sensor data, is also performed to compare the respective values with those obtained using the analytical modeling.

4.1 Spectral analysis

Spectral analysis is a qualitative non-parametric analysis technique that is used frequently to determine the vibration periods of structures. The technique involves the determination of transmissibility functions in order to aid in the determination of the modal periods of the bridge. Transmissibility functions (Ljung 1987, Pandit 1991) express the relationship between recorded input acceleration for a structure and the recorded output acceleration of the structure

$$S_{yx}(\omega) = H(i\omega)S_{xx}(\omega), \quad S_{yy}(\omega) = H(i\omega)S_{xy}(\omega) \quad (2)$$

where ω is the frequency of vibration; $S_{xx}(\omega)$, $S_{yy}(\omega)$ denote the power spectral density (PSD) functions; $S_{xy}(\omega)$, $S_{yx}(\omega)$ denote the cross power spectral density (CPSD) functions; and $H(i\omega)$ is the transmissibility function. It must be noted that $S_{xy}(\omega)$ and $S_{yx}(\omega)$ are complex conjugates. Typically, the two estimates of the transmissibility function presented in Eq. (3) obtained by rearranging Eq. (2) slightly differ due to presence of noise and leakage associated with the discrete Fourier transform

$$H_1(i\omega) = \frac{S_{yx}(\omega)}{S_{xx}(\omega)}, \quad H_2(i\omega) = \frac{S_{yy}(\omega)}{S_{xy}(\omega)} \quad (3)$$

The periodogram estimation technique (Oppenheim 1989) is used to estimate the PSD and CPSD functions and the transmissibility function is derived as described in Eq. (3). The technique involves performing Fast Fourier Transform (FFT) of several overlapping segments of the signal. The periodogram is then computed as the average of the square of the FFT amplitudes over the segments and may therefore be visualized as a procedure to smoothen the Fourier spectrum of the recorded data. The absolute value or the magnitude of the transmissibility function, $H(i\omega)$ is called the transmissibility factor (TF), and the frequency at the maximum TF is the fundamental frequency of vibration of the structure. The ratio of the imaginary and real components of $H(i\omega)$

gives the tangent of the phase angle between the input and output signals. The phase angle essentially varies between $-\pi$ and $+\pi$ radians.

Figs. 5(a) and 5(b) show the plot of TF versus frequency for the Meloland Road Overpass and Painter Street Overpass, respectively, while Figs. 5(c) and 5(d) show the plot of phase angle versus frequency. Clearly it is seen that the phase angles vary between $-\pi$ and $+\pi$ radians for both bridges. Table 1 shows a comparison of the first two modal vibration periods obtained using the analytical model and spectral analysis. Also shown are results from some of the previous studies on these bridges. It is seen that in general there is a very good agreement between the results. Figs. 6(a)~6(c) show the fundamental mode shapes for the case study bridges. The fundamental mode is

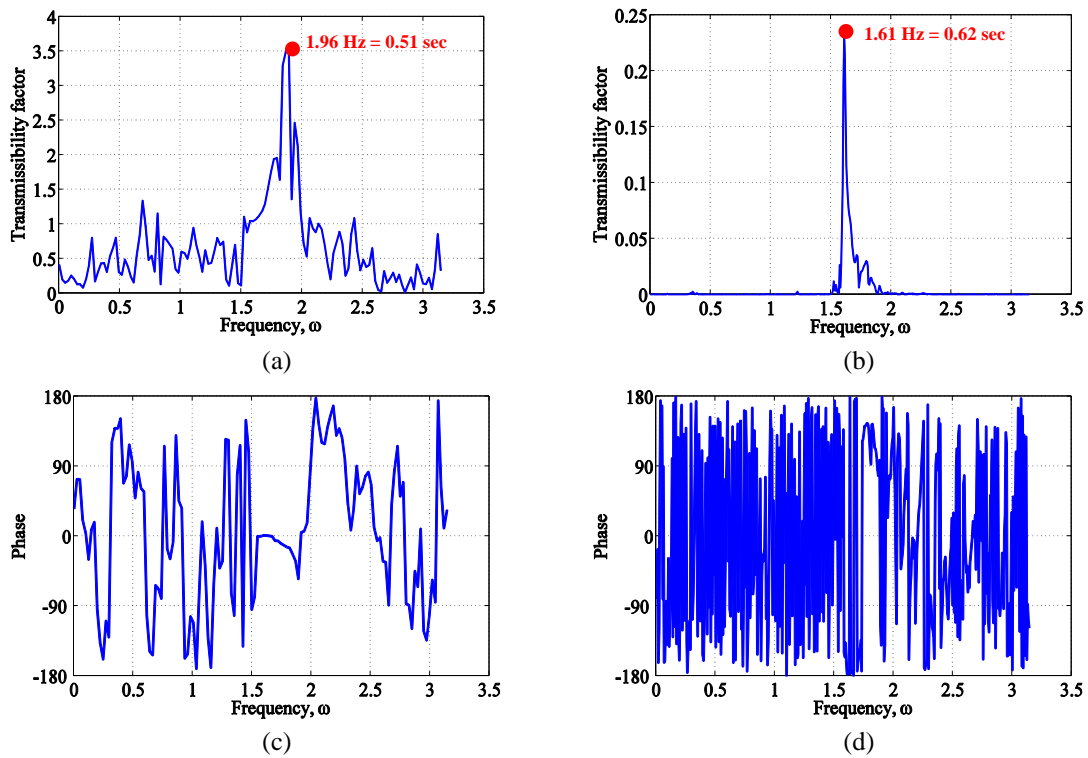


Fig. 5 Plot of TF versus frequency for (a) Meloland Road Overpass and (b) Painter Street Overpass; plot of phase angle versus frequency for (c) Meloland Road Overpass and (d) Painter Street Overpass

Table 1 Comparison of modal vibration periods (sec) from spectral analysis and analytical model

Bridge	Analytical model		Spectral analysis		Previous studies	Mode-1	Mode-2
	Mode-1	Mode-2	Mode-1	Mode-2			
Meloland Road Overpass	0.46	0.35	0.51	0.38	Zhang and Makris (2002)	0.49	0.35
					Kwon and Elnashai (2008)	0.32	0.31
					Werner <i>et al.</i> (1987)	0.39	-
Northwest Connector	1.58	1.44	1.56	1.30	DesRoches and Fenves (1997)	1.56	1.30
					Liu <i>et al.</i> (1996)	1.89	1.67
Painter Street Overpass	0.52	0.48	0.62	0.54	Zhang and Makris (2002)	0.56	0.44

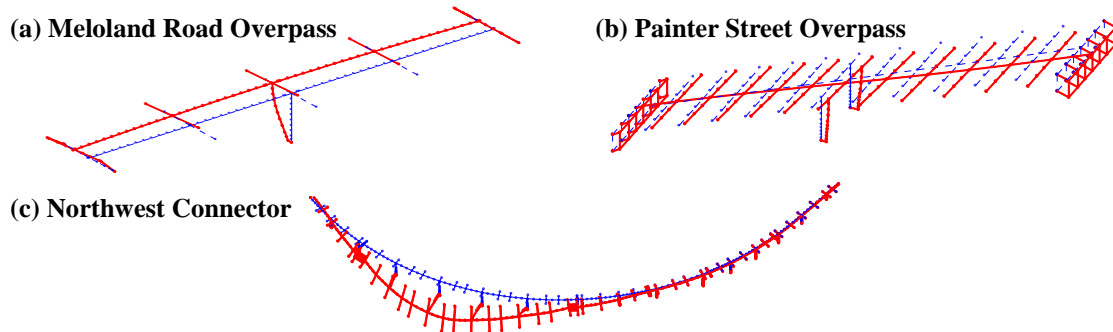


Fig. 6 Fundamental mode shapes for the case study bridges

in the transverse direction for the Meloland Road Overpass and the Northwest Connector while it involves a coupled longitudinal and transverse mode for the Painter Street Overpass.

4.3 Response comparison: analytical model and recorded sensor data

Figs. 7(a) and 7(b) show the sensor layout for the Meloland Road Overpass and Painter Street Overpass, respectively. The sensor layout for the Northwest Connector was already shown in Fig. 2.

NLTHA was conducted on the analytical bridge models using the respective scenario bi-directional time histories recorded at the bridge sites. The longitudinal and transverse directions of the Meloland Road Overpass are subjected to the 1979 Imperial Valley earthquake with PGA values of 0.31 g and 0.29 g, respectively. The 1992 Cape Mendocino/Petrolia earthquake is used in the case of the Painter Street Overpass and is characterized with PGA values of 0.28 g and 0.52 g in the longitudinal and transverse directions, respectively. In the case of the Meloland and Painter Street Overpass, uniform excitation (acceleration time histories) was imposed while in the case of the Northwest Connector, multi-support excitation (displacement time histories) was imposed.

Multi-support excitation plays a very important role in the case of long span bridges where the probability of the input motion being coherent and synchronous at all supports is greatly reduced. It includes the spatial variability of ground motions and random incoherence, difference in the local soil conditions, and wave propagation across the site (DesRoches and Fenves 1997, Lupoi *et al.* 2005). The ground motions were not recorded at the base of every column in the connector, and therefore the input motion for each column was based on the nearest recorded motion without interpolation; for example, the input motions for Bent 7 were imposed using the ground motions recorded at the footing of Bent 8. The 1992 Landers earthquake is used for analytical model validation of the Northwest Connector. Table 2 provides details about the ground motions and their locations used in the multi-support excitation analysis for the Northwest Connector.

Comparisons between the analytical model results and recorded real time sensor data were performed across all sensors (channels) and the comparisons for a few channels on the case study bridges are shown in Figs. 8, 9, and 10. The responses shown in these figures pertain to critical locations on the bridges along with an effort to present responses across a range of components. Figs. 8(a) and 8(b) show the response comparison for abutments and deck in the transverse direction, respectively, for the Meloland Road Overpass: Channels 3 and 7. The channels selected for the Northwest Connector: 20, 28, and 29, are all located close to the longitudinal center of the

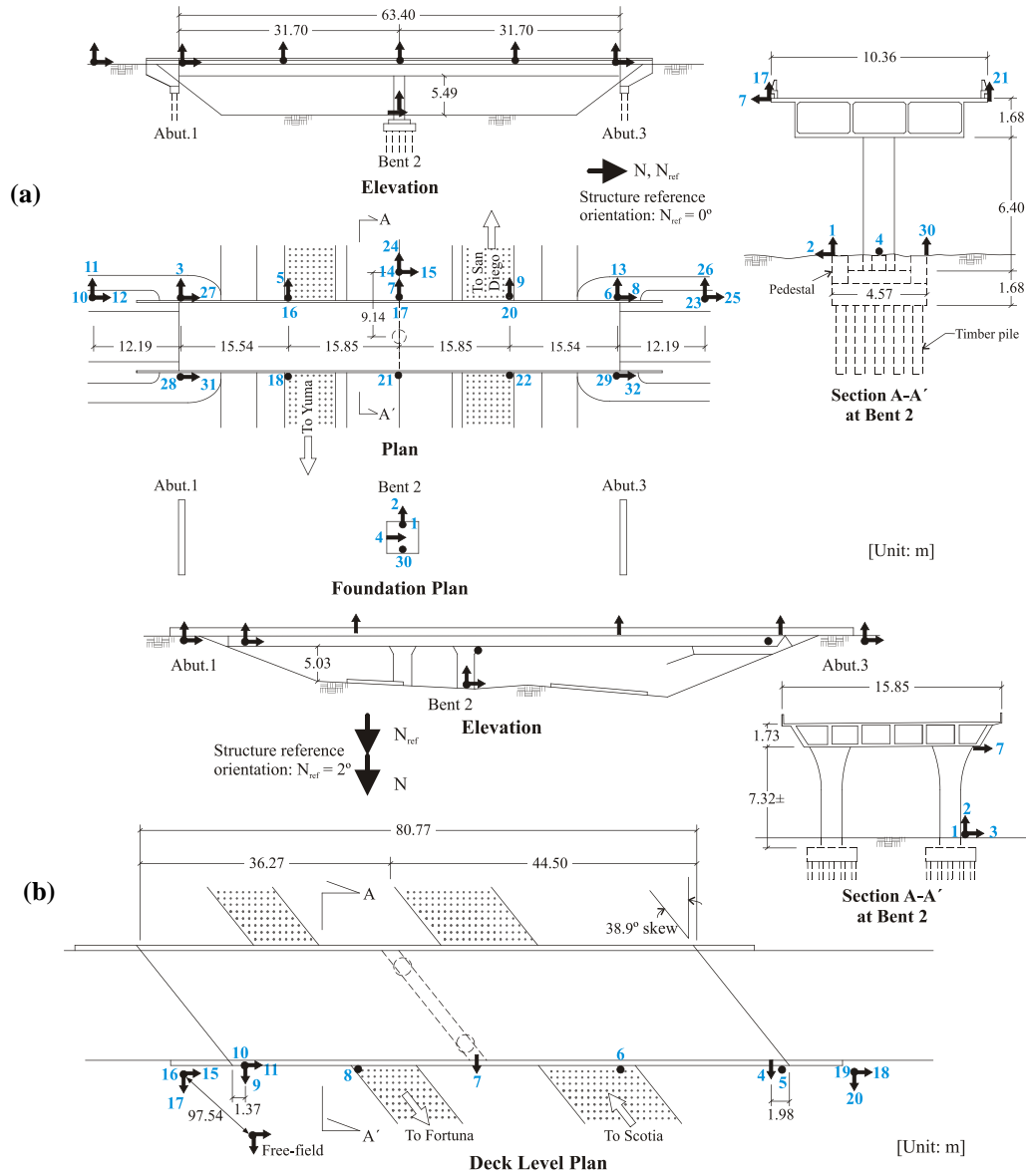


Fig. 7 Plan, elevation and sectional views of the (a) Meloland Road Overpass and (b) Painter Street Overpass, showing the sensor layout

Connector and Figs. 9(a), 9(b), and 9(c) show the response of the deck at Hinges 7 and 11, respectively. These figures present the comparison of displacement responses between uniform excitation and multi-support excitation to investigate the effect of non-uniform ground motion on their responses. The input ground motions selected in this study are those recorded at Bent 8 which is located near the center of the bridge. Although the uniform excitation analysis produces reasonable estimates at Channels 20 and 28, it overestimates the transverse displacement amplitude of the deck at Channel 29. On the other hand, the multi-support excitation analysis

Table 2 Details of the ground motions used in FEM validation of the Northwest Connector

Ground motion number	Location on bridge	Peak ground displacement (mm)		
		Longitudinal	Transverse	Vertical
1	Abutment 1	82.0	49.0	25.9
2	Bent 3	70.6	60.5	-
3	Bent 8	34.0	124.0	28.2
4	Abutment 17	83.3	80.3	26.2

correlates well with the recorded sensor data for all three channels. This comparison emphasizes the importance of considering multi-support excitation including the spatial variability of ground motions for long bridges in better estimating their seismic demand. Figs. 10(a), 10(b), and 10(c) compare the displacement responses of the analytical results and recorded sensor data at Channels 4, 11, and 7, respectively. Channels 4 and 11 recording the response of the abutments in the transverse and longitudinal directions, respectively, were chosen for the Painter Street Overpass along with Channel 7, which show the transverse deck displacement. It can be seen that there is a very good agreement in all cases thereby demonstrating the accuracy and superiority of three dimensional modeling techniques.

5. Component response and relative vulnerability

This section provides some insights into the response of bridge components using deterministic analysis performed for the scenario earthquakes that each of the case study bridges was subjected to. The relative shift in vulnerability among bridge components is investigated by developing fragility curves for each of the case study bridges.

Fig. 11(a) shows the column response of the Meloland Road Overpass in the transverse direction when subjected to the 1979 Imperial Valley earthquake. The maximum moment of the column is 3,886 kN-m resulting in a curvature of approximately 0.00055 m^{-1} . Another potential way of assessing the response is by considering alternate metrics such as curvature ductility demand, defined as the ratio of the maximum curvature in the column cross-section due to the

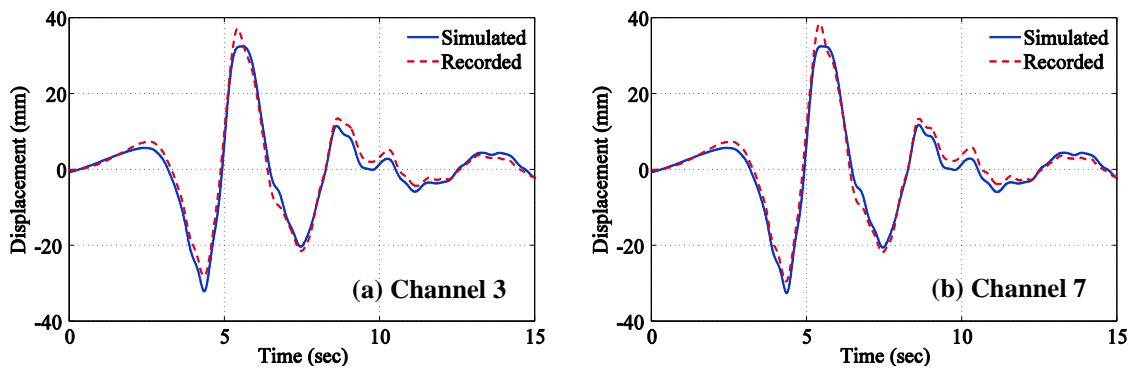


Fig. 8 Comparison of responses from the analytical model and sensor data for the Meloland Road Overpass

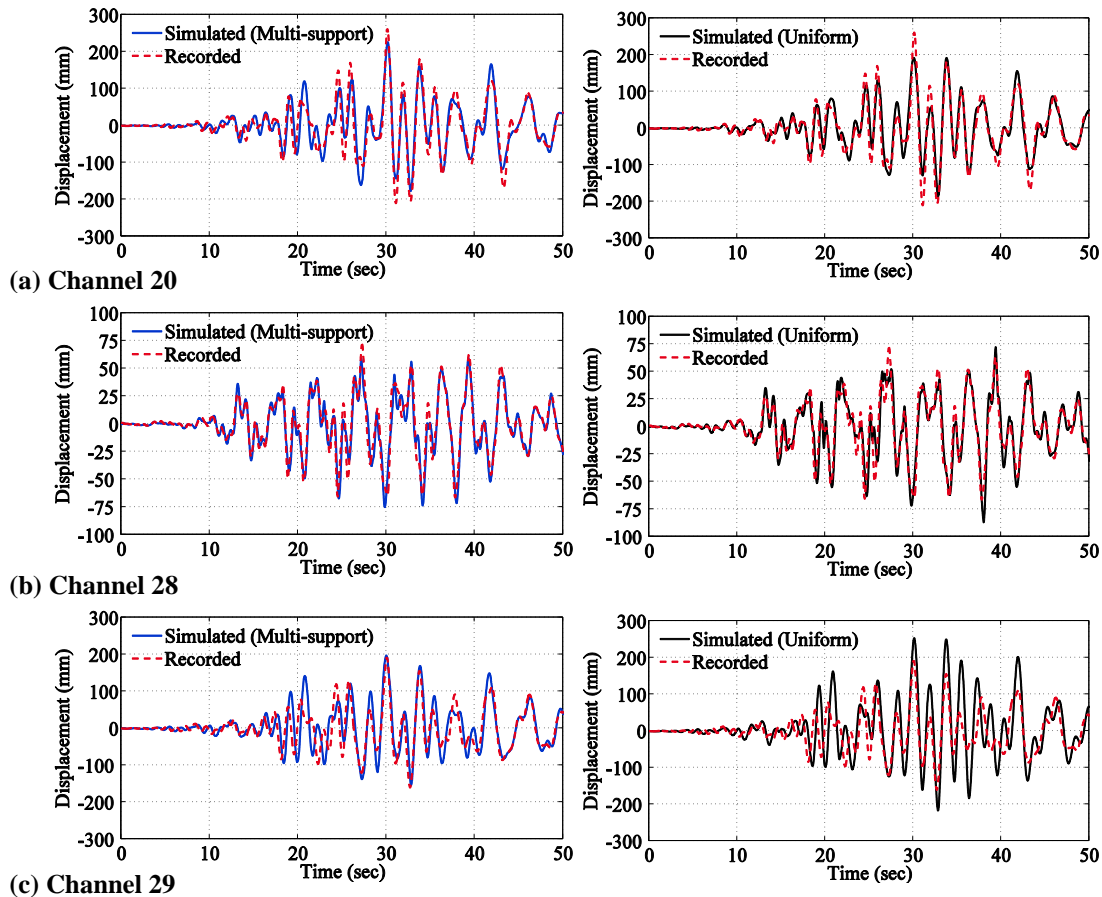


Fig. 9 Comparison of responses from the analytical model and sensor data for the Northwest Connector

imposed earthquake load to the curvature that causes first yield of the outermost rebar. The yield curvature was determined based on a moment-curvature analysis and found to be 0.00305 m^{-1} . The transverse curvature ductility demand was found to be 0.18, which is less than one indicating that the column remains elastic. This is consistent with the observation during the earthquake where no damage was evident on the bridge column. Fig. 11(b) shows the longitudinal response of the abutments. It is evident that the abutment deforms 11 mm in both active and passive directions and clearly the tensile response is a matter of concern since it could cause serious damage to the piles. This is expected in diaphragm-type abutments where both active and passive actions tend to engage in contrary to seat-type abutments where passive action is engaged to a greater extent due to pounding action between the deck and the abutment back wall. In this case, the active response is critical when compared to the passive response since the horizontal resistance is offered solely by the piles when the abutment is pulled away from the backfill. Choi (2002) assumed the limit states for abutments in active action to occur at deformations of 4 mm, 8 mm, 25 mm, and 51 mm, for slight, moderate, extensive, and complete damage states, respectively. These values correspond to half the first yield, first yield, ultimate and twice the ultimate deformation, respectively. In this case, the active response leads to moderate damage and is the same with the transverse response.

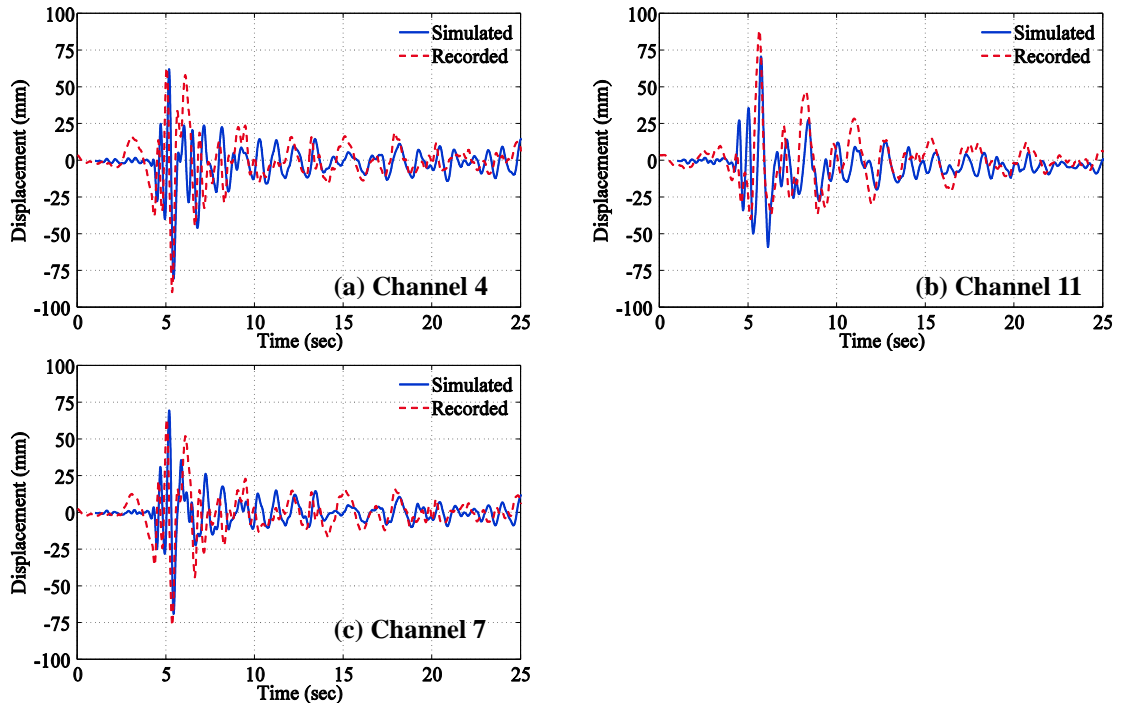


Fig. 10 Comparison of responses from the analytical model and sensor data for the Painter Street Overpass

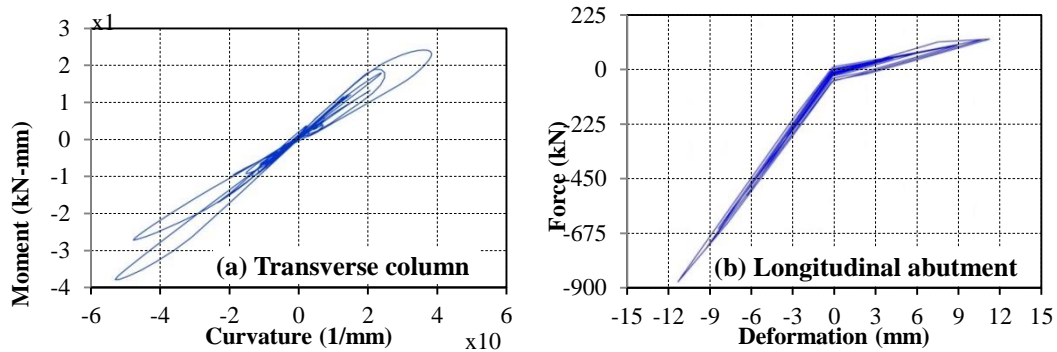


Fig. 11 Component responses of Meloland Road Overpass under the Imperial Valley earthquake

As will be demonstrated later in the section, these two components tend to dominate the overall vulnerability of the Meloland Road Overpass at the system level.

Fig. 12(a) illustrates the column response of the Northwest Connector in the transverse direction when subjected to the 1992 Landers earthquake. Bent 8 might be more vulnerable under seismic excitation in comparison to other bents due to a lack of retrofit and further its proximity to the longitudinal center of the bridge. The maximum moment at Bent 8 is in the order of 32,760 kN-m at a curvature of about 0.00091 m^{-1} . The yield curvature was found to be 0.00252 m^{-1} using section analysis. As in the case of Meloland Road Overpass, the transverse curvature ductility demand was 0.36 which is less than one and therefore, the column remains elastic. DesRoches and

Fenves (1997) indicated that there was no evidence of damage to the column during the earthquake. Fig. 12(b) shows the longitudinal response of Abutment 1 and the abutment deforms 73 mm and 30 mm in the active and passive directions, respectively. As mentioned previously in the case of Meloland Road Overpass, the longitudinal response of abutments reemphasizes that the tensile (active) response is very important for bridges with diaphragm-type abutments. In accordance with the limit states proposed by Choi (2002), the active response of Abutment 1 may lead to moderate damage. Intermediate hinges tend to be a vulnerable component because of the possibility of unseating due to its opening and closing during seismic excitation. Fig. 12(c) indicates the response of hinge opening and closing including the effect of the cable restrainers at Hinge 3 during the same earthquake. The initial restrainer cable slack and the gap of expansion joint were assumed to be 13 mm and 25 mm, respectively, as proposed by DesRoches and Fenves (1997). The maximum hinge opening and closing were found to be 62 mm and 29 mm, respectively. Post-earthquake inspection indicated that the seat of Hinge 3 had three hairline cracks radiating from the reentrant corner of the seat. Although there was no observed damage to the cable restrainers, concrete spalling and reinforcing bar exposure on the inside edge of the deck near Hinge 3 were observed (DesRoches and Fenves 1997). The opening and closing movements of the hinge due to repeated loadings may lead to slight or moderate damage. The hysteretic response of elastomeric bearing pad at Hinge 3 is shown in Fig. 12(d). Unlike other components, the elastomeric bearing underwent inelastic response. The elastomeric bearing pad, 711 mm×305 mm×140 mm in dimension, underwent a maximum deformation of 61 mm. The yield displacement was assumed to be 10% of the thickness of the bearing pad, as illustrated in Section 3.2 of the paper. The ratio of the maximum deformation to the yield displacement is about 4.4 and therefore

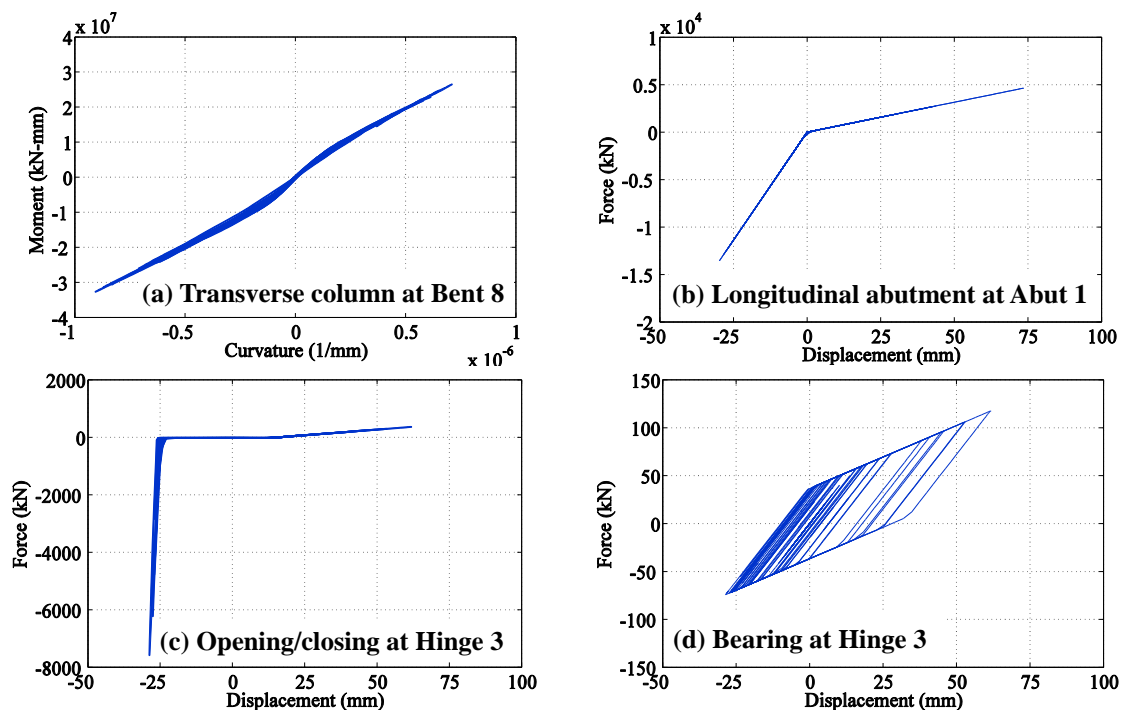


Fig. 12 Component responses of Northwest Connector under the Landers earthquake

the bearing might be subjected to moderate damage although this was not directly observed in the post-earthquake inspection due to its location in the bridge. While the steel jacketing on the columns and footings made these components less vulnerable at the system level, the active component of abutment response, hinge opening and elastomeric bearing pads may have experienced moderate damage. These three components tend to dominate the overall vulnerability of the Northwest Connector at the system level.

Fig. 13(a) presents the column moment-curvature response of the Painter Street Overpass in the transverse direction when excited by the 1992 Cape Mendocino/Petrolia earthquake. It is clear from the figure that the maximum column curvature is 0.00252 m^{-1} corresponding to a moment of 8,236 kN-m. As in the previous case studies, the column yield curvature is found to be 0.00343 m^{-1} from section analysis and it corresponds to a curvature ductility demand of 0.73. The column remains elastic under this excitation which is consistent with past bridge observation where no damage was

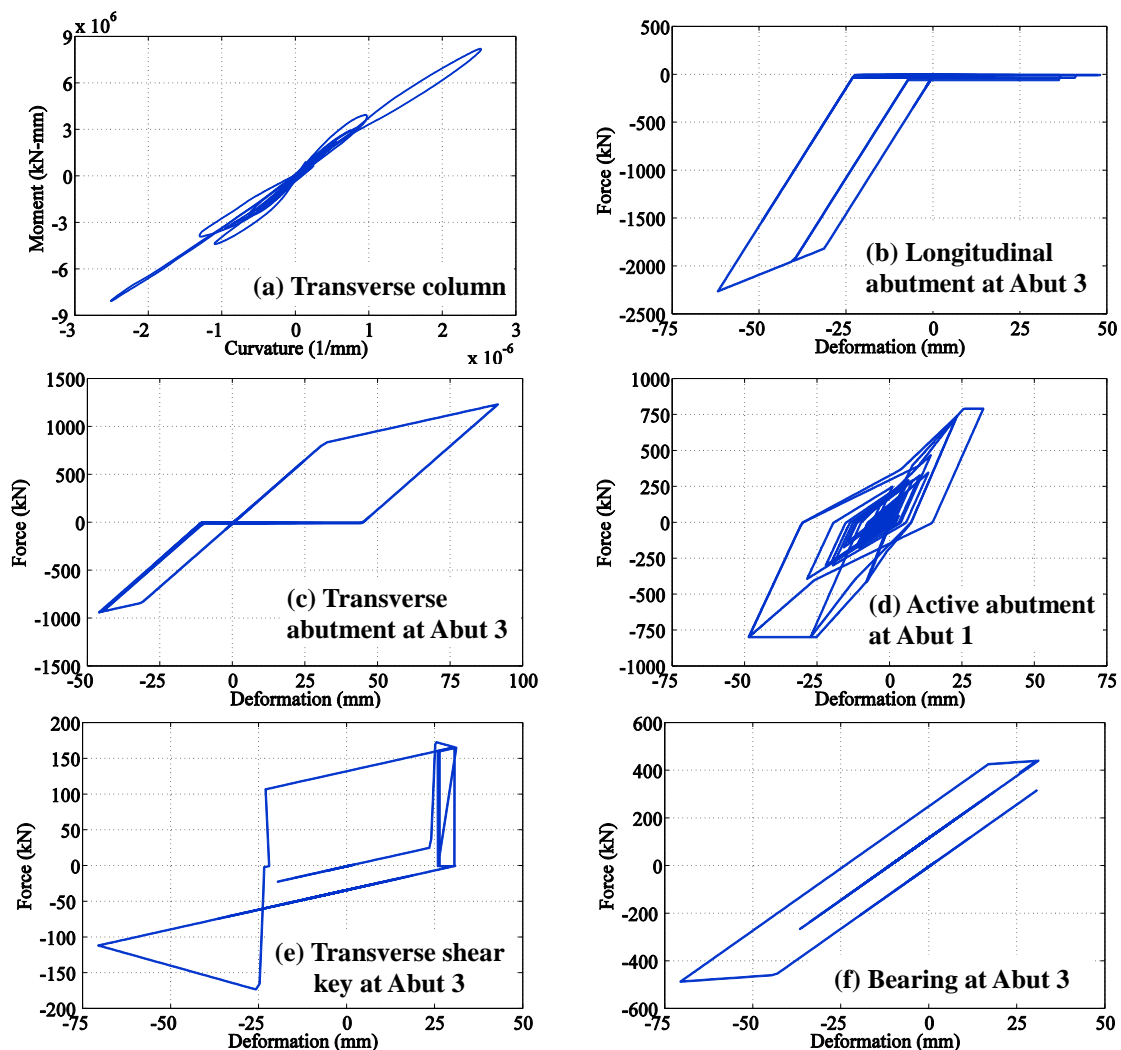


Fig. 13 Component responses of Painter Street Overpass under the Cape Mendocino/Petrolia earthquake

evident on the bridge columns. The presence of skew typically leads to a complex coupled response of the bridge and this is evident in the case of the Painter Street Overpass where the abutments record comparable displacements in both longitudinal and transverse directions. As shown in Figs. 13(b) and 13(c), Abutment 3 experiences displacements of 62 mm and 91 mm in the longitudinal and transverse directions, respectively. Additionally, these comparable displacements may be attributed to the fact that the deck and the abutments are monolithic. This is further demonstrated in case of Abutment 1 which records an active displacement of 49 mm, as shown in Fig. 13(d). In accordance with the limit states proposed by Choi (2002), the active response of Abutment 1 may cause moderate damage to the abutment. Unlike the Meloland Road Overpass and the Northwest Connector, the Painter Street Overpass has wing walls in both east and west abutments and therefore the transverse capacity of the abutments is not dominated by the piles. Therefore, the same limit states are considered for both the longitudinal and transverse directions. Per these limit states, Abutment 3 experiences slight damage in the transverse direction.

The bridge has shear keys in Abutment 3 in both longitudinal and transverse directions. Fig. 13(e) shows the transverse response of the shear key at Abutment 3. Based on the response, it may be concluded that the shear key approaches its ultimate capacity and experiences a displacement of 71 mm which corresponds to moderate damage. This is consistent with observations reported by Shamsabadi *et al.* (2010). Abutment 3 also has an elastomeric bearing pad on top of the pile cap, 380 mm wide and 76 mm thick. Based on the force-deformation response of the bearing shown in Fig. 13(f), it is seen that the maximum bearing deformation is 71 mm which translates to slight damage. Consistent with these observations, it is seen that the active response of the abutments and shear keys dominate the overall vulnerability of the bridge system.

5.1 Insights into the behavior of curved and skewed bridges

The aim of this section is to provide some insight into the performance of curved and skewed bridges based on assimilation of the analytical models and dynamic analyses presented in the prior sections. Curved bridge columns are subjected to multi-directional deformation with torsion due to the coupling of the longitudinal and transverse response, thereby making them susceptible to complex flexural and shear failures. Furthermore, there is likelihood for significant nonlinearity at the expansion joint associated with the slippage and pounding between the girders. The response might be different based on the ground motion intensity.

Fig. 14 shows a schematic of a typical expansion joint in a curved bridge comprising elastomeric bearing pads, shear key, and restrainers. The opening of the expansion joint is associated with the deformation of the elastomeric bearing pads under shear thereby offering resistance to motion. This continues eventually leading to their slippage when the maximum friction force is mobilized. The restrainers engage to resist the opening of the joint when the relative joint displacement equals the initial slack and the resistance builds up linearly until the restrainer cables yield. The same happens during the closing of the joint except that the restrainer cables do not engage and pounding between the adjacent slabs and girders takes place when the joint completely closes. The joint response is unsymmetrical and the magnitude of joint opening and closure and the associated radially inward and outward motion of the bridge depend on the intensity of the ground motion. During small intensity earthquakes, it is likely that pounding between the girders will not take place since the relative displacement at the joint is below the initial joint gap. In this case, the elastomeric bearing pads and restrainers alone resist the joint separation and as such small or no displacement response may be expected in the radially outward

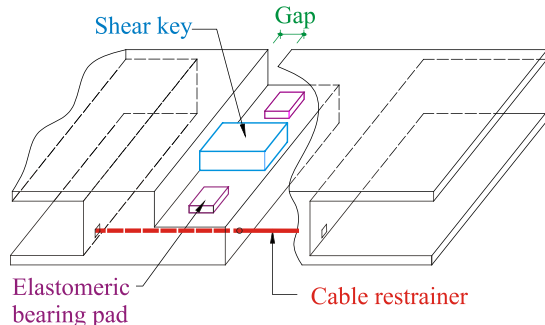


Fig. 14 Typical bridge expansion joint

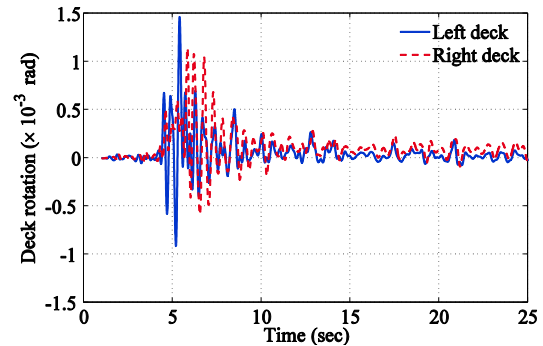


Fig. 15 Rotation about the vertical axis for the left and right decks in the Painter Street Overpass

direction of the bridge. On the other hand, during high intensity ground motions, significant pounding and yielding of the restrainer cables may be expected leading to increased response in the radially outward direction of the bridge due to arching action between the abutments.

Similar to curved bridges, skewed bridges exhibit unique response to seismic excitations due to strut action which causes rotation of the superstructure due to pounding between the deck and the abutment. In multi-span bridges, the stiffness of the bent may differ on either side of the skewed deck leading to differential transverse displacements, thereby causing rotation of the superstructure and associated pounding. Fig. 15 shows the rotation about the vertical axis for the left and right decks.

The response predicted by linear analysis in which the expansion joint is idealized by a set of linear springs will significantly differ from that predicted by the analytical models in the present study which accounts for the effects of impact, slippage and yielding of the restrainer cables. Likewise, simplistic models neglecting the effect of pounding will not provide a good correlation with the actual response of the bridge subject to seismic excitations. It is imperative to correctly idealize the structural integrity of the bridge by accounting for nonlinear component effects to realistically predict the response of bridges with complex geometries.

5.2 Fragility and relative vulnerability

A common technique to compare the relative vulnerability among bridge components and account for uncertainty in the performance assessment is to derive fragility curves. Fragility curves serve as an excellent tool to study the effects of uncertainty propagated through the system and the probabilities of exceeding different user-defined damage states. Furthermore, the relative contribution of various bridge components to the overall system vulnerability can be assessed. This information is typically not available through deterministic analyses as illustrated in the previous section. Bridge system and component level fragility curves are developed for each of the case study bridges in accordance with the procedure adopted by Ramanathan *et al.* (2010, 2011). Uncertainties are considered in the material properties: concrete compressive strength and reinforcing steel yield strength, in addition to the seismic hazard. A suite of one hundred recorded ground motions were used for generating the curves. 80 recorded ground motions in California identified by Medina and Krawinkler (2003) were extracted from the Pacific Earthquake Engineering Research (PEER) Center's Strong Motion Database and used along with 20 ground

Table 3 Bridge component limit states

Component	EDP	Units	Slight		Moderate		Extensive		Complete	
			S_C^*	β_C^*	S_C	β_C	S_C	β_C	S_C	β_C
Column (as-built)	Curvature ductility	N.A.	1.44	0.25	2.70	0.25	3.92	0.47	4.18	0.47
Column (retrofit)	Curvature ductility	N.A.	9.35	0.25	17.7	0.25	26.1	0.47	30.2	0.47
Abutment - passive	Displacement	mm	38	0.25	146	0.25	1000	0.47	1000	0.47
Abutment - active	Displacement	mm	10	0.25	38	0.25	76	0.47	1000	0.47
Abutment - transverse	Displacement	mm	10	0.25	38	0.25	76	0.47	1000	0.47
Abutment - transverse (Painter)	Displacement	mm	38	0.25	146	0.25	1000	0.47	1000	0.47
In-span hinge	Displacement	mm	76	0.25	102	0.25	152	0.47	254	0.47
Elastomeric bearing	Displacement	mm	29	0.25	104	0.25	136	0.47	187	0.47
Elastomeric bearing (Painter)	Displacement	mm	76	0.25	114	0.25	152	0.47	269	0.47
Shear key	Displacement	mm	25	0.25	76	0.25	152	0.47	356	0.47

* S_C and β_C are the median value and dispersion of limit states, respectively

motions pertinent to Los Angeles from the SAC project database. The 80 PEER ground motions have an even selection of recorded time histories from four bins that include combinations of low and high moment magnitudes, large and small epicentral distances. The magnitudes vary between 5.8 and 6.9 while the epicentral distances vary between 10 km and 60 km. The suite of twenty SAC ground motions for Los Angeles have ten pairs each with intensities of 2% and 10% probability of exceedence in 50 years, respectively. The bridge component engineering demand parameters (EDPs) considered and their prescriptive limit state values are shown in Table 3 and these are consistent with those found in Ramanathan *et al.* (2010, 2011). As mentioned in the previous section, in the case of the Painter Street Overpass, the presence of wing walls and skew in the superstructure leads to a coupled response and hence the limit states for both passive and transverse response of the abutments are assumed to be the same, as listed in Table 3. The bearing limit states for the Painter Street Overpass are consistent with those presented in Padgett and DesRoches (2008). Shear strains of 100%, 150%, and 200% are assumed for slight through extensive limit states, corresponding to slight damage, yielding of steel shims, and severe bending of steel shims in the bearings of the Painter Street Overpass, respectively. Shear deformation dominates the limit states up to extensive damage while sliding in the bearings dictates the capacity thereon. The limit state for the complete damage state is defined as half of the bearing support length of 356 mm in this case.

Fig. 16 shows the bridge system and component level fragility curves for the three case study bridges for a few representative damage states. In every case, it is assumed that multiple components contribute to the overall vulnerability of the bridge system. Response of columns and abutments in the longitudinal (passive and active actions) and transverse directions are considered as components of interest in all the cases. Additionally, elastomeric bearing pads, in-span hinges and shear keys are considered in the case of the Northwest Connector and Painter Street Overpass. Figs. 16(a) and 16(b) show the fragility curves at the bridge system and component level for the Meloland Road Overpass at the two intermediate damage states: moderate and extensive. It is seen that transverse and active response of the abutments dominates the overall vulnerability

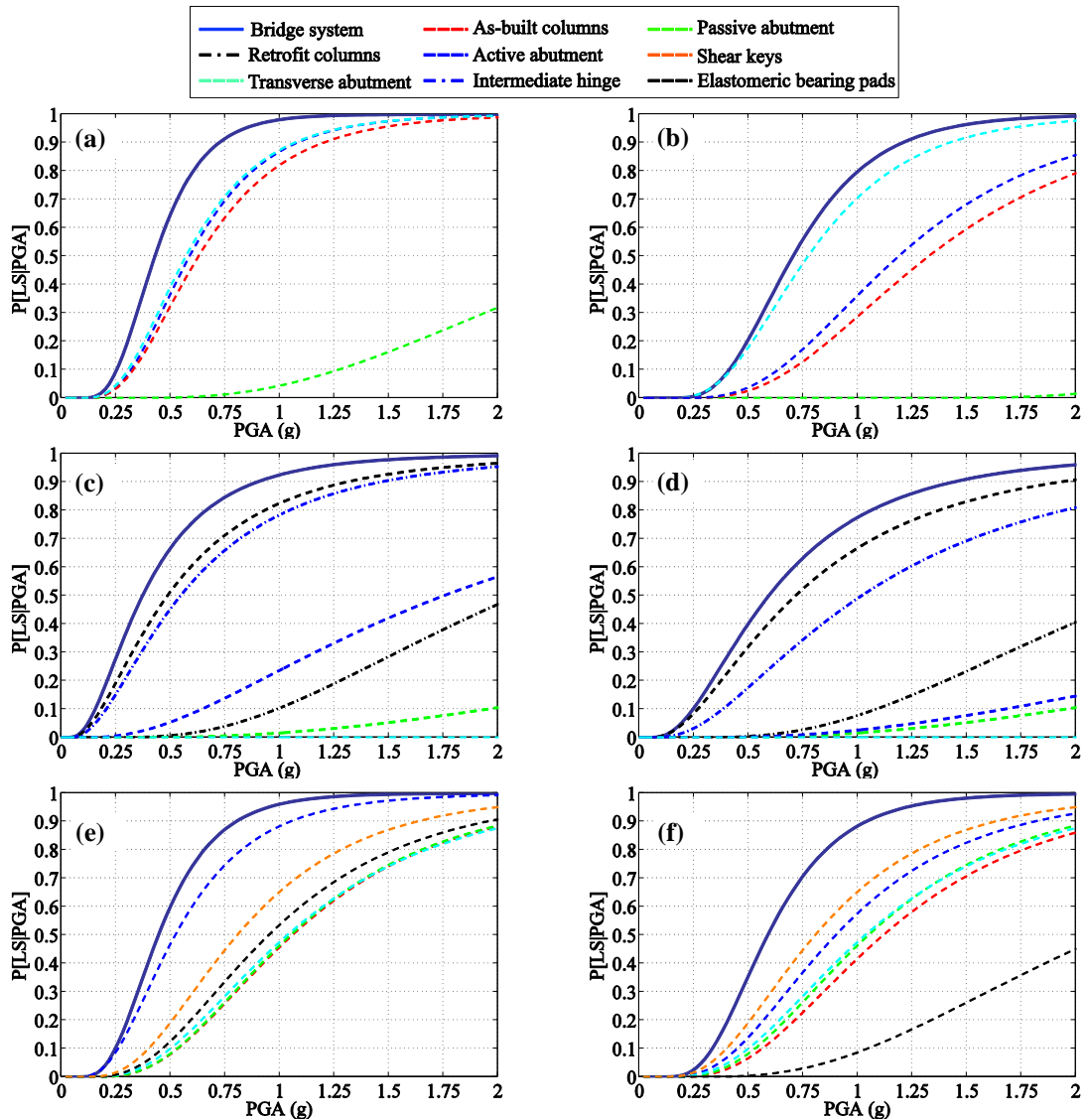


Fig. 16 Bridge system and component level fragility curves for a) Meloland Road Overpass at moderate damage state, b) Meloland Road Overpass at extensive damage state, c) Northwest Connector at extensive damage state, d) Northwest Connector at complete damage state, e) Painter Street Overpass at extensive damage state, and f) Painter Street Overpass at complete damage state

at the system level. This is consistent with the observations in the previous section when excessive demand was seen imposed on either of these responses. It should be noted that the bridge as a system is more fragile than any one of its components as a consequence of the underlying series assumption that was used in the system fragility formulation. The component fragility curves for the Northwest Connector at the higher damage states: extensive and complete, are shown in Figs. 16(c) and 16(d). The elastomeric bearings tend to be the most vulnerable component in this case followed by intermediate hinges, as discussed in the previous section. As in the case of the

Meloland Road Overpass, the active abutment response dominates the system vulnerability in the case of Painter Street Overpass followed by the shear keys (Figs. 16e and 16f).

6. Conclusions

The fundamental focus of this paper is to present modeling considerations and insight into the performance of three instrumented multi-span continuous concrete box-girder bridges in California. Meloland Road Overpass, Northwest Connector, and Painter Street Overpass are chosen as the case study bridges and detailed description is provided about the analytical modeling procedure, and key considerations for straight, curved, and skewed bridges. Although this study does not aim to provide explicit design guidelines for these structures, the identification of vulnerable components in bridges with curved and skewed superstructures can support designers by highlighting critical areas of concern for bridges with these complex yet relatively common geometries. Three dimensional nonlinear finite element models are developed in each case and a detailed description is provided regarding the modeling considerations and associated assumptions. The responses from the analytical models are compared with recorded sensor data for scenario earthquakes specific to individual bridges made available through the Center for Engineering Strong Motion Data to test the robustness of the modeling and dynamic analysis procedures. Uniform support excitation was adopted in the case of the Meloland Road and Painter Street Overpasses while multi-support excitation was used in the case of the Northwest Connector to account for the random incoherence and spatial variability of ground motions due to its long bridge length. Spectral analysis is employed to identify fundamental frequencies from sensor data recorded during real time earthquakes and these are compared to the results from the modal analysis of analytical models. Component and system level fragility curves are developed to assess the component vulnerabilities using a suite of one hundred ground motions that represent the seismic hazard in the region to provide additional insight into the uncertainty and probabilities of exceeding a few user-defined bridge system level damage states.

The following are some of the conclusions drawn from the present study:

- The analytical models yield comparable responses to the sensor data available for the case study bridges. This reflects the efficacy of the modeling and analysis techniques.
- The fundamental mode is in the transverse direction for the Meloland Road Overpass and the Northwest Connector, while it is a coupled longitudinal and transverse mode for the Painter Street Overpass. The corresponding time periods are 0.46 sec, 1.58 sec, and 0.52 sec, respectively. There is a very good agreement between these results and those obtained by using Spectral Analysis.
- Response of abutments in active action and transverse direction was seen to be critical in the case of the Meloland Road Overpass. This is attributed to the presence of monolithic abutments in this bridge. Furthermore, these components dominate the overall vulnerability of the bridge system as demonstrated by developing fragility curves. Analysis reveals potential slight to moderate damage to the abutments but this was not reported probably due to lack of access for inspection.
- In the case of the Northwest Connector, elastomeric bearing pads are found to be the most vulnerable components followed by the response of the intermediate hinges. This is consistent with past earthquake damage where hair line cracks radiating from the reentrant corner of the seat was observed. The analysis reveals moderate damage to the bearings, but this was not reported in the post-earthquake inspection potentially due to the location of the bearings in the bridge and difficulties associated with the inspection.

- Active response of the abutments and shear key response dominate the overall vulnerability of the Painter Street Overpass. The analysis reveals comparable abutment displacements in the longitudinal and transverse directions. This is attributed in part to the coupled response due to the presence of skew in the superstructure and being characterized by diaphragm type abutments.

References

- Abdel-Mohti, A. and Pekcan, G. (2008), "Seismic response of skewed RC box-girder bridges", *Earthq. Eng. Eng. Vib.*, **7**(4), 415-426.
- ACI (2008), "Building code requirements for structural concrete (ACI 318-08) and commentary", American Concrete Institute, Farmington Hills, MI.
- Basoz, N. and Kiremidjian, A. (1998), "Evaluation of bridge damage data from the Loma Prieta and Northridge, California earthquakes", Multidisciplinary Center for Earthquake Research, University at Buffalo, NY, Technical Report MCEER-98-0004.
- Bignell, J.L., LaFave, J.M. and Hawkins, N.M. (2005), "Seismic vulnerability assessment of wall pier supported highway bridges using nonlinear pushover analyses", *Eng. Struct.*, **27**(14), 2044-2063.
- Bjornsson S., Stanton L. and Eberhard M. (1998), Seismic response of skew bridges", *6th U.S. National Conference on Earthquake Engineering*, Seattle, WA.
- Buckle, I.G., Friedland, I., Mander, J., Martin, G., Nutt, R. and Power, M. (2006), "Seismic retrofitting manual for highway structures: Part 1-bridges", Multidisciplinary Center for Earthquake Research, University at Buffalo, NY, Technical Report MCEER-06-SP10.
- Caltrans (2010), "Seismic design criteria version 1.6", California Department of Transportation, Division of Engineering Services, Office of Structure Design, Sacramento, CA.
- Choi, E. (2002), "Seismic analysis and retrofit of Mid-America bridges", Ph.D. Dissertation, Georgia Institute of Technology, Atlanta.
- DesRoches, R. and Fenves, G.L. (1997), "Evaluation of recorded earthquake response of a curved highway bridge", *Earthq. Spectra*, **13**(3), 363-386.
- Dimitrakopoulos, E.G. (2010), "Analysis of a frictional oblique impact observed in skew bridges", *Nonlinear Dyn.*, **60**, 575-595.
- Douglas, B.M. and Richardson, J. (1984), "Maximum amplitude tests of a highway bridge", *8th World Conference on Earthquake Engineering*, San Francisco, CA.
- Douglas, B.M. Maragakis, E A., Vrontino, S. and Douglas, B.J. (1990), "Analytical studies of the static and dynamic response of the Meloland Road Overcrossing", *4th US National Conference on Earthquake Engineering*, Vol. 1, Palm Springs, CA.
- Fenves, G.L., Filippou, F.C. and Sze, D.T. (1992), "Response of the Dumbarton Bridge in the Loma Prieta earthquake", Earthquake Engineering Research Center, University of California, Berkeley, CA, Report No. UCB/EERC-92/02.
- Fenves, G.L. and Ellery, M. (1998), "Behavior and failure analysis of a multiple-frame highway bridge in the 1994 Northridge earthquake", Pacific Earthquake Research Center, University of California, Berkeley, CA, Report No. PEER 98/08.
- Gates, J.H. and Smith, M.J. (1982), "Verification of dynamic modeling method by prototype excitation", California Department of Transportation, Office of Structures Design, Sacramento, CA, Report No. FHWA/CA/SD-82/07.
- Goel, R.K. and Chopra, A.K. (1997), "Evaluation of bridge abutment capacity and stiffness during earthquakes", *Earthq. Spectra*, **13**(1), 1-23.
- Haddadi, H., Shakal, A., Stephens, C., Savage, W., Huang, M., Leith, W., Parrish, J. and Borchardt, R. (2008), "Center for Engineering Strong-Motion Data (CESMD)", *14th World Conference on Earthquake Engineering*, Beijing, China.
- Huang, M.J. and Shakal, A.F. (1995), "CSMIP strong-motion instrumentation and records from the I10/215

- interchange bridge near San Bernardino”, *Earthq. Spectra*, **11**(2), 193-215.
- Kaviani, P., Zareian, F. and Sarraf, M. (2010), “Comparison of seismic response of skewed bridges to near vs. far field motions”, *7th International Conference on Urban Earthquake Engineering & 5th International Conference on Earthquake Engineering*, Tokyo, Japan.
- Kwon, O.-S. and Elnashai, A.S. (2008), “Seismic analysis of Meloland Road Overcrossing using multiplatform simulation software including SSI”, *J. Struct. Eng.*, **134**(4), 651-660.
- Liu, W.D., Kartoum, A., Dhillon, S., Chen, X. and Imbsen, R.A. (1996), “Implications of the strong-motion records from a retrofitted curved bridge on seismic design and performance”, *SMIP96 Seminar on Seismological and Engineering Implications of Recent Strong-Motion Data*, California Geological Survey, pp. 71-88.
- Ljung, L. (1987), “System identification”, Prentice-Hall, Englewood Cliffs, NJ.
- Lupoi, A., Franchin, P., Pinto, P.E. and Monti, G. (2005), “Seismic design of bridges accounting for spatial variability of ground motion”, *Earthq. Eng. Struct. Dyn.*, **34**(4-5), 10-25.
- McCallen, D.B. and Romstad, K.M. (1994), “Dynamic analyses of a skewed short-span, box-girder overpass”, *Earthq. Spectra*, **10**(4), 729-755.
- Ma, Y. and Deng, N. (2000), *Deep foundations*, in Bridge Engineering Handbook, eds., W.-F. Chen and L. Duan, CRC Press LLC.
- Mander, J.B., Priestley, M.J.N. and Park, R. (1988), “Theoretical stress-strain model for confined concrete”, *J. Struct. Eng.*, **114**(8), 1804-1826.
- Maroney, B., Romstad, K. and Chajes, M. (1990), “Interpretation of Rio Dell freeway response during six recorded earthquake events”, *4th US National Conference on Earthquake Engineering*, Vol. 1, Palm Springs, CA.
- Maroney, B., Kutter, B., Romstad, K., Chai, Y.H. and Vanderbilt, E. (1994), “Interpretation of large scale bridge abutment test results”, *3rd Annual Seismic Research Workshop*, Sacramento, CA.
- McKenna, F., Scott, M.H. and Fenves, G.L. (2010), “Nonlinear finite-element analysis software architecture using object composition”, *J. Comput. Civ. Eng.*, **24**(1), 95-107.
- Medina, R.A. and Krawinkler, H. (2003), “Seismic demands for nondeteriorating frame structures and their dependence on ground motions”, John A. Blume Earthquake Engineering Center, Stanford University, CA, Report No. 144.
- Megally, S.H., Silva, P.F. and Seible, F. (2002), “Seismic response of sacrificial shear keys in bridge abutments”, Dept. of Structural Engineering, University of California, San Diego, CA, Report No. SSRP-2001/23.
- Meng, J.Y. and Lui, E.M. (2000), “Seismic analysis and assessment of a skew highway bridge”, *Eng. Struct.*, **22**(11), 1433-1452.
- Moehle J., Fenves, G., Mayes, R., Priestley, N., Seible, F., Uang, C.-M., Werner, S. and Aschheim, M. (1995), “Highway bridges and traffic management”, *Earthq. Spectra*, **11**(S2), 287-372.
- Naeim, F. and Kelly, J.M. (1999), *Design of seismic isolated structures: from theory to practice*, John Wiley & Sons, Inc., New York.
- Muthukumar, S. and DesRoches, R. (2006), “A Hertz contact model with non-linear damping for pounding simulation”, *Earthq. Eng. Struct. Dyn.*, **35**(7), 811-828.
- Oppenheim, A.V. and Schaffer, R.W. (1989), *Discrete-time signal processing*, Prentice-Hall, Englewood Cliffs, NJ.
- Padgett, J.E. and DesRoches, R. (2008), “Methodology for the development of analytical fragility curves for retrofitted bridges”, *Earthq. Eng. Struct. Dyn.*, **37**(8), 1157-1174.
- Pandit, S.M. (1991), *Modal and spectrum analysis*, John Wiley, New York.
- Priestley, M.J.N., Seible, F. and Calvi, G.M. (1996), *Seismic design and retrofit of bridges*, John Wiley & Sons, Inc., New York.
- Priestley, M.J.N., Seible, F., Xiao, Y. and Verma, R. (1994), “Steel jacket retrofitting of reinforced concrete bridge columns for enhanced shear strength-Part 1: theoretical considerations and test design”, *ACI Struct. J.*, **91**(4), 394-404.
- Ramanathan, K., DesRoches, R. and Padgett, J.E. (2010), “Analytical fragility curves for multispan

- continuous steel girder bridges in moderate seismic zones”, *J. Trans. Res. Board*, **2202**(3), 173-182.
- Ramanathan, K., DesRoches, R. and Padgett, J.E. (2011), “A comparison of pre- and post-seismic design considerations on moderate seismic zones through the fragility assessment of multispan bridge classes”, *Eng. Struct.*, **45**, 559-573.
- Romstad, K., Kutter, B., Maroney, B., Vanderbilt, E., Griggs, M. and Chai, Y.H. (1995), “Experimental measurements of bridge abutment behavior”, University of California, Davis, CA, Report No. UCD-STR-95-1.
- Shamsabadi, A., Khalili-Tehrani, P., Stewart, J.P. and Taciroglu, E. (2010), “Validated simulation models for lateral response of bridge abutments with typical backfills”, *J. Bridge Eng.*, **15**(3), 302-311.
- Stewart, J.P., Taciroglu, E., Wallace, J.W., Ahlberg, E.R., Lemnitzer, A., Rha, C., Tehrani, P.K., Keowan, S., Nigbor, R.L. and Salamanca, A. (2007), “Full scale cyclic testing of foundation support systems for highway bridges. Part II: Abutment backwalls”, University of California, Los Angeles, CA, Report No. UCLA-SGEL-2007/02.
- Sweet, J. and Morrill, K.B. (1993), “Nonlinear soil-structure interaction simulation of the Painter Street Overcrossing”, *2nd Annual CALTRANS Seismic Research Workshop*, Sacramento, CA.
- Werner, S.D., Beck, J.L. and Levine, M.B. (1987), “Seismic response evaluation of Meloland Road Overpass using 1979 Imperial Valley earthquake records”, *Earthq. Eng. Struct. Dyn.*, **15**(2), 249-274.
- Wilson, J.C. and Tan, B.S. (1990a), “Bridge abutments: formulation of simple model for earthquake response analysis”, *J. Eng. Mech.*, **116**(8), 1828-1837.
- Wilson, J.C. and Tan, B.S. (1990b), “Bridge abutments: assessing their influence on earthquake response of Meloland Road Overpass”, *J. Eng. Mech.*, **116**(8), 1838-1856.
- Yashinsky, M. and Ostrom, T. (2000), “Caltrans’ new seismic design criteria for bridges”, *Earthq. Spectra*, **16**(1), 285-307.
- Zhang, J. and Makris, N. (2002), “Seismic response analysis of highway overcrossings including soil structure interaction”, *Earthq. Eng. Struct. Dyn.*, **31**(11), 1967-1991.